Eur. Phys. J. Spec. Top. (2023) 232:649–654
https://doi.org/10.1140/epjs/s11734-022-00712-5

THE EUROPEAN PHYSICAL JOURNAL SPECIAL TOPICS

Regular Article

Multiscale entropy and fluctuation analyses of complex signals

A. N. Pavlov[1,2,a] and O. N. Pavlova[1]

[1] Saratov State University, Astrakhanskaya Str. 83, 410012 Saratov, Russia
[2] Regional Scientific and Educational Mathematical Center "Mathematics of Future Technologies", 410012 Saratov, Russia

Received 24 August 2022 / Accepted 26 October 2022 / Published online 7 November 2022

Abstract A coarse-graining procedure that averages the original dataset over non-overlapping time windows of increased duration was earlier proposed as part of the multiscale entropy (MSE) computation algorithm. This idea of coarse-grained time series can be used to quantify other features of time series. Here we discuss the application of two methods, MSE and an extended version of detrended fluctuation analysis (DFA) to coarse-grained datasets associated with both simulated and experimental signals. We show that the coarse-graining procedure can improve the diagnostics of changes in the system dynamics performed using extended DFA compared to the MSE method.

1 Introduction

Analysis of complex signals is typically carried out by decomposing them into simpler components that are easier to process and characterize. Thus, methods using the Fourier transform decompose signals into sets of harmonic functions quantified by magnitudes, frequencies, and phase shifts [1]. The analytical signal approach, based on the Hilbert transform or its enhancement [2, 3], introduces the instantaneous amplitudes and frequencies of non-harmonic oscillations and allows their independent analysis, which also simplifies the interpretation of changes occurring in the dynamics under study. Another type of decomposition is signal filtering, which is applied within the framework of various data processing techniques [4–6]. When the system involves independent or weakly coupled mechanisms that produce rhythmic contributions in distinct frequency ranges, the use of band-pass filtering improves their performance. The latter is important, e.g., for studying the electrical activity of the brain, electroencephalograms, where α, β, γ and other rhythms reflect various states of the body: relaxation, sleep, concentration, etc. The independence of these rhythmic contributions enables to separate them by means of band-pass filters with appropriate cutoff frequencies. For the time-varying dynamics of physiological systems, adaptive filtering is often used, and multiresolution wavelet analysis [7, 8] based on a discrete wavelet transform with orthogonal basic functions, such as the Daubechies family [9], is one of the fairly popular tools for studying signal features in non-overlapping frequency ranges. This tool makes it possible to predict the bifurcations of complex regimes from transients before their visual recognition or identification by means of standard signal processing approaches. The latter is important to diagnose pathological changes in physiology. Moreover, the pyramidal decomposition algorithm ensures the speed of computations, which is often a necessary circumstance.

A simple filtering variant is the "coarse-graining" procedure described in [10–12], where multiple time series are created by averaging datasets in non-overlapping time windows. By increasing the length of the window, it becomes possible to cover a wide range of scales. In [10–12] this approach was applied to compute the multiscale entropy (MSE). Entropy-based approaches are often considered to characterize the dynamics of complex systems, including Shannon entropy [13], Kolmogorov-Sinai entropy, approximate entropy (ApEn) [14], sample entropy (SampEn) [15], etc. The ApEn quantifies the irregularity or randomness of data sets depending on two values, the pattern length and the tolerance factor. Although it can be applied to experimental signals, it has restrictions in the case of short and noisy data. A modified approach, the SampEn was designed to address the main restrictions of ApEn regarding the amount of data and inconsistent results. The capabilities of SampEn are described in several works, e.g. [15, 16]. The MSE method uses SampEn to quantify the complexity of signals as a function

[a] e-mail: pavlov.alexeyn@gmail.com (corresponding author)

of the time scale. This method has found various applications in physiological data due to its adaptation to characterize the hierarchical complexity of natural processes.

Coarse-grained time series can be used in a wider range of possible applications of signal processing techniques, not limited to complexity measures only. In particular, they are suitable for quantifying the correlation properties of time series over a certain range of scales. The purpose of this paper is to compare MSE analysis with fluctuation analysis [17–20] of coarse-grained time series using both simulated and experimental data to characterize the broader possibilities of the coarse-graining procedure for diagnostics. Our study will begin with the interactive dynamics of two coupled benchmark models of nonlinear dynamics, Lorenz models producing chaotic oscillations, where transitions across the boundary of the synchronization region change the properties of signals, and the associated changes are reflected in different characteristics, including complexity and predictability. Next, we discuss the experimental data of relative cerebral blood flow (CBF) acquired in rats using laser speckle contrast analysis [21, 22]. We show that scaling exponents of extended detrended fluctuation analysis (extended DFA or EDFA) [19, 20], which is a modified DFA approach for the case where nonstationarity varies throughout the signal, can provide a better recognition of changes in the dynamics compared to complexity measures.

The paper is organized as follows. In Section 2, we briefly consider the coarse-graining procedure and two methods, MSE and EDFA. This section also describes the models and datasets considered for analysis. The main results of the comparison of multiscale entropy and fluctuation analyses are given in Section 3. The conclusions of the study are summarized in Section 4.

2 Methods

2.1 Coarse-graining procedure

Multiple coarse-grained time series $y_j(\tau)$ [10–12] are obtained by averaging the original data set x_i, $i = 1, \ldots, N$ within time windows that do not overlap and have increased duration τ

$$y_j^\tau = \frac{1}{\tau} \sum_{i=(j-1)\tau+1}^{j\tau} x_i, \quad 1 \le j \le N/\tau. \tag{1}$$

The length of y_j^τ reduces as τ increases.

2.2 Multiscale entropy

The MSE was recently elaborated to characterize the complexity of natural processes according to its intuitive definition [23]. It was shown that this method has advantages over other entropy-based measures which quantify complexity in general, i.e. without any reference to specific frequency bands or time scales [10–12]. The MSE improves the interpretation of observed changes in complexity as it provides a link between such changes and time scales associated, e.g., with various physiological control mechanisms. This approach uses SampEn and computes it for every scale factor value.

After obtaining multiple coarse-grained time series $y_j(\tau)$, SampEn (S_E) is estimated for each of them. This quantity is proportional to the logarithm of the probability of maintaining similarity between patterns of length m and $m + 1$ for two series of data points. Within this approach, self-matches are not taken into account when estimating the probability (see [10] for more details). The works [11, 12] used a wide range of scales. When dealing with relatively short datasets or the time-varying dynamics of complex systems, the range of scales is reduced since a reliable computation of probabilities cannot be done as the scale factor increases due to the shortening of $y_j(\tau)$. In the current work, we applied the MSE software developed by M. Costa (https://www.physionet.org) [24].

2.3 Extended detrended fluctuation analysis

Extended detrended fluctuation analysis (EDFA) [19, 20] represents a modified version of the original approach developed by Peng et al. [17, 18] which was widely used in various fields [25–29]. Its peculiarity is the consideration of the case when nonstationarity varies throughout the signal, and an additional measure is introduced to take into account such behavior. As part of the DFA method applied to the x_i time series, a signal profile is built

$$z_k = \sum_{i=1}^{k} x_i, \tag{2}$$

separated into non-overlapping segments of length n, and the local (usually, linear) trend z_k^n is estimated within each segment by the least squares algorithm. Root-mean-square fluctuations around z_k^n often show a power-law dependence

$$F(n) = \sqrt{\frac{1}{N} \sum_{k=1}^{N} [z_k - z_k^n]^2} \sim n^\alpha \tag{3}$$

with a scaling exponent α, which quantitatively determines the features of anti-correlated ($\alpha < 0.5$) or correlated ($\alpha > 0.5$) dynamics of complex systems.

If the nonstationarity changes throughout the entire signal, then the inhomogeneity of trend features can be described by the measure

$$\sigma(F_{loc}(n)) \sim n^\beta \tag{4}$$

which quantifies how the distribution of local RMS fluctuations $F_{loc}(n)$ of the signal profile from the trend

varies with the segment length n [30, 31]. The power-law behavior of $\sigma(F_{loc}(n))$ is described by a scaling exponent β, which is different from α. Nearly stationary datasets are quantified by negative values of β. For the time-varying dynamics of natural systems, this measure takes positive values.

2.4 Simulated data

To investigate the cooperative dynamics of coupled chaotic oscillators, a system of two interacting Lorenz models was chosen. The equations for each unit represent the benchmark model of nonlinear dynamics, which is used for studying the mechanisms of chaos formation and destruction [32]

$$\begin{aligned} \frac{dx_{1,2}}{dt} &= s(y_{1,2} - x_{1,2}) + \gamma(x_{2,1} - x_{1,2}), \\ \frac{dy_{1,2}}{dt} &= r_{1,2}x_{1,2} - x_{1,2}z_{1,2} - y_{1,2}, \\ \frac{dz_{1,2}}{dt} &= x_{1,2}y_{1,2} - z_{1,2}b, \end{aligned} \tag{5}$$

The parameter set s =10, r_1 =28.8, r_2 =28, and b =8/3 defines the dynamics of the units, γ is the strength of interaction. As signals for further processing, the sequences of return times into the secant plane $x_1^2+y_1^2 = 30$ and $x_2^2 + y_2^2 = 30$ were used. According to the work [33], the model (5) shows an atypical phenomenon, namely, initial desynchronization with the growth of γ (in the range $\gamma \in [0.0, 2.0]$. At $\gamma > 2$, the oscillation frequencies of the interacting units are adjusted in accordance with the expected dynamics of the coupled systems.

2.5 Experimental data

Relative CBF velocity acquired by laser speckle contrast analysis [21, 22] was used. Experimental procedures were carried out at the Saratov State University on 9 adult male rats in accordance with the "Guide for the Care and Use of Laboratory Animals". Recordings of the duration 10 minutes were made after adaptation to environmental conditions (30 min). Two physiological states were considered: background and pharmacologically induced hypertension caused by the administration of mesaton (Sigma) at a dose of 0.5 μg/kg. The second recording was made 10 minutes after the injection. The existence of physiological protecting mechanisms avoids significant changes in CBF measured in veins and arteries, but reactions in the capillary network may occur. For studying the effects of such hypertension, a He-Ne laser (Thorlabs HNL210L, 632.8 nm) was chosen to illuminate the cerebral cortex, and measurements of speckle patterns were carried out with a Basler acA2500-14gm CMOS camera (sampling rate 40 frames/s). Contrast was evaluated by definition $K=\sigma/\langle I\rangle$, where σ is the standard deviation and $\langle I\rangle$ is the mean intensity averaged over a window of 5×5 pixels. The velocity of relative CBF was measured as a value inversely proportional to K [34, 35]. The study [19] showed stronger responses in small cerebral vessels to acute increase of peripheral blood flow. Due to this, measurements in capillaries were carried out as an integral assessment of a speckle image window in the vicinity of a large vessel.

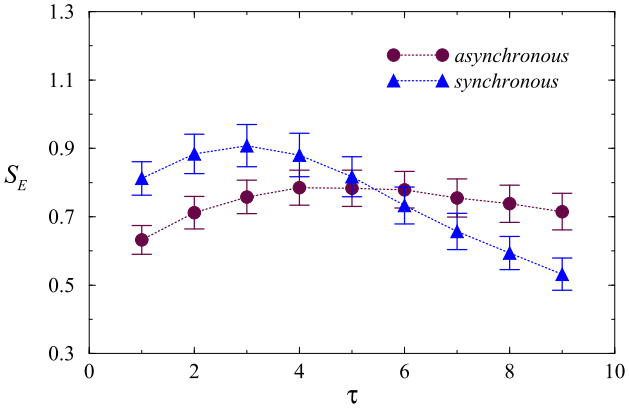

Fig. 1 Multiscale entropy estimated for synchronous and asynchronous dynamics of two interacting Lorenz models

3 Results and discussion

3.1 Simulated data

Chaotic synchronization typically changes the structure of signals produced by interacting nonlinear systems with self-sustained oscillations. In addition to the adjustment of basic frequencies, phase locking and other phenomena related to time scales or frequencies, chaotic synchronization can change the complexity, predictability and correlation features of signals produced by coupled units. This is illustrated in Fig. 1, where the different behavior of S_E with growing scale factor for synchronous and asynchronous dynamics makes it possible to distinguish between such types of chaotic behavior of interacting Lorenz models. With the exception of the initial segments of the dependencies shown in Fig. 1, the values of S_E decrease with increasing τ, but the decay of $S_E(\tau)$ is stronger for synchronous chaotic oscillations.

Analysis of the correlation properties using the α exponent of the conventional DFA (Fig. 2a) does not give noticeable distinctions between the dynamics under study at large τ, although at small values of the scale factor, both types of complex oscillations show a different behavior, namely, anticorrelations ($\alpha < 0.5$) for synchronous dynamics and positive correlations ($\alpha > 0.5$) for asynchronous regime. The adjustment of α values with growing τ does not ensure their reliable separation (Fig. 2a), but the β exponent of the extended method (EDFA) exhibits a different behavior (Fig. 2b) and reveals stronger distinctions compared to S_E and α. The latter confirms that the application of methods

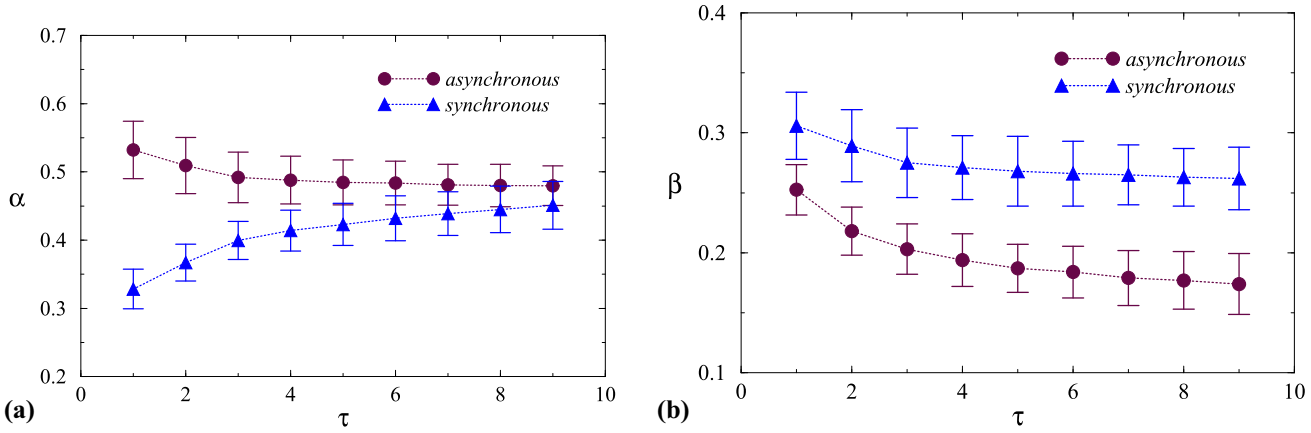

Fig. 2 Scaling exponents α (**a**) and β (**b**) depending on the scale factor for synchronous and asynchronous oscillations in a system of coupled Lorenz models. Here, β shows better diagnostic results compared to α and S_E (see Fig. 1)

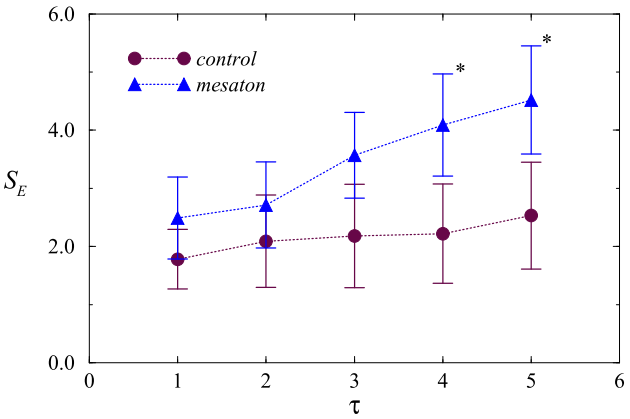

Fig. 3 Multiscale entropy of experimental datasets for background dynamics (control) and pharmacologically induced hypertension (mesaton). Stars show significant distinctions between the states (the Mann-Whitney test, $p < 0.05$)

other than the multiscale entropy to multiple coarse-grained time series represents a useful signal processing approach.

3.2 Experimental data

Unlike simulated datasets, the analysis of experimental time series is restricted by their length, which limits the available range of the scale factor, and is complicated by the nonstationary behavior of natural systems that also creates additional difficulties in reliably interpreting the results of signal processing. Nevertheless, the application of both approaches, MSE and EDFA, makes it possible to reveal the effects of acute peripheral hypertension on the dynamics of microcerebral blood flow in the capillary network. In the example under consideration, the use of multiscale entropy analysis makes it possible to distinguish between background dynamics and pharmacologically induced hypertension caused by the administration of mesaton (Fig. 3) for scale factors $\tau > 3$ ($p < 0.05$ according to the Mann-Whitney test).

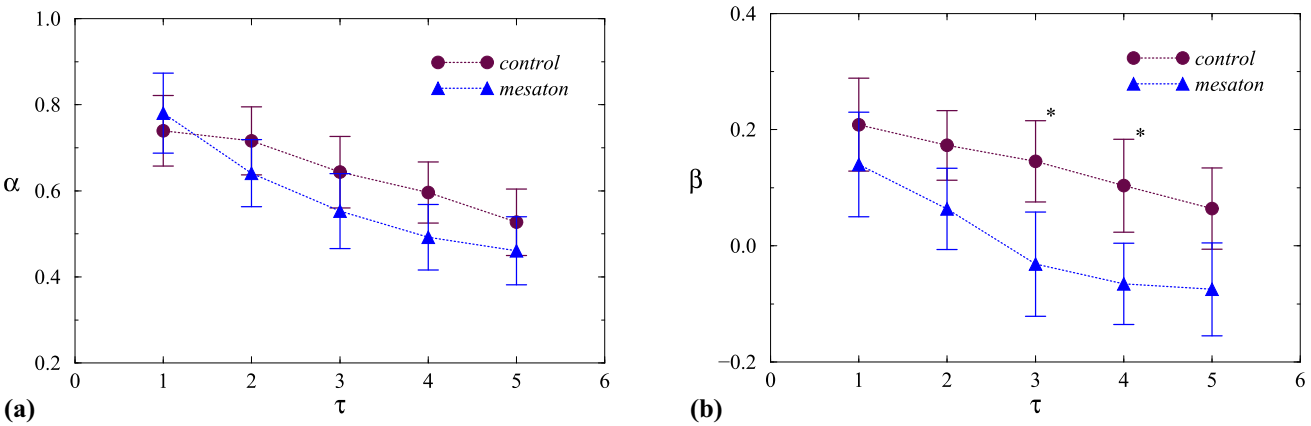

Fig. 4 Scaling exponents α (**a**) and β (**b**) depending on the scale factor for experimental datasets. Stars show significant distinctions between the states (the Mann-Whitney test, $p < 0.05$)

Applying EDFA to these datasets shows less noticeable distinctions for the α exponent (Fig. 4a). The latter may be explained by the mentioned limitation of the amount of data and the related length of the region of long-range correlations. Distinctions in the time-varying dynamics of the micro-vascular network quantified by the β exponent are more pronounced than for the α exponent (Fig. 4b), and are comparable with the MSE method, although significant differences ($p < 0.05$ according to the Mann-Whitney test) are detected at other values of τ (3 and 4). Thus, the use of coarse-grained time series within various signal processing techniques makes it possible to more thoroughly analyze complex dynamics and improve the diagnosis of changes in the system behavior. This analysis can be applied to various fields of research, including physiology [36–38], physics [39–41], engineering [42, 43], energetics [44, 45], etc.

4 Conclusion

In the current study, we considered the application of two approaches, MSE and EDFA to coarse-grained datasets related to simulated and experimental signals. Using sequences of return times into the Poincare section for a system of two interacting Lorenz models, we showed how the scaling exponent of EDFA can outperform diagnostics of transitions between different states compared to the MSE method. Similar diagnostic results are shown for relative CBF velocity in microcerebral blood vessels during an acute increase in peripheral blood pressure (pharmacologically induced hypertension). The results confirm that the coarse-graining procedure may have more opportunities for signal processing in various fields.

Acknowledgements The authors acknowledge O.V. Semyachkina-Glushkovskaya and A.S. Abdurashitov for their interest in this work, experimental data and valuable discussions. This work was supported by the Russian Science Foundation (Agreement 19-12-00037).

Data availability statement The datasets generated during and/or analysed during the current study are available from the corresponding author on reasonable request.

References

1. J.S. Bendat, A.G. Piersol, *Random data: analysis and measurement procedures, 4th Edition*. Wiley, (2010)
2. N.E. Huang, Z. Shen, S.R. Long, M.C. Wu, H.H. Shih, Q. Zheng, N.C. Yen, C.C. Tung, H.H. Liu, Proc. R. Soc. Lond. A **454**, 903 (1998)
3. N.E. Huang, S.S.P. Shen, *Hilbert-Huang Transform and its Applications*. World Scientific, (1995)
4. S. Thurner, M.C. Feurstein, M.C. Teich, Phys. Rev. Lett. **80**, 1544 (1998)
5. B.B. Hubbard, *The World according to wavelets: the story of a mathematical technique in the making, 2nd Edition*. CRC Press, (1998)
6. P.S. Addison, *The Illustrated Wavelet Transform Handbook: Introductory Theory and Applications in Science, Engineering, Medicine and Finance, 2nd Edition*. CRC Press, (2017)
7. Y. Meyer, *Wavelets: Algorithms & Applications*. Soc. Ind. Appl. Math. (1993)
8. S. Mallat, *A wavelet tour of signal processing: the sparse way, 3rd Edition*. Academic Press, (2008)
9. I. Daubechies, *Ten Lectures on Wavelets*. Soc. Ind. Appl. Math. (1992)
10. M. Costa, A.L. Goldberger, C.-K. Peng, Phys. Rev. E **71**, 021906 (2005)
11. M. Costa, A.L. Goldberger, C.-K. Peng, Phys. Rev. Lett. **89**, 062102 (2002)
12. M. Costa, C.-K. Peng, A.L. Goldberger, J.M. Hausdorff, Phys. A **330**, 53 (2003)
13. C.E. Shannon, Bell Sys. Tech. J. **27**, 379 (1948)
14. S.M. Pincus, Proc. Natl. Acad. Sci. **88**, 2297 (1991)
15. J.S. Richman, J.R. Moorman, Am. J. Physiol. Heart Circ. Physiol. **278**, H2039 (2000)
16. D.E. Lake, J.S. Richman, M.P. Griffin, J.R. Moorman, Am. J. Physiol. Regul. Integr. Comp. Physiol. **283**, R789 (2002)
17. C.-K. Peng, S.V. Buldyrev, S. Havlin, M. Simons, H.E. Stanley, A.L. Goldberger, Phys. Rev. E **49**, 1685 (1994)
18. C.-K. Peng, S. Havlin, H.E. Stanley, A.L. Goldberger, Chaos **5**, 82 (1995)
19. A.N. Pavlov, A.S. Abdurashitov, A.A. Koronovskii Jr., O.N. Pavlova, O.V. Semyachkina-Glushkovskaya, J. Kurths, Commun. Nonlin. Sci. Numer. Simulat. **85**, 105232 (2020)
20. A.N. Pavlov, A.I. Dubrovsky, A.A. Koronovskii Jr., O.N. Pavlova, O.V. Semyachkina-Glushkovskaya, J. Kurths, Chaos **30**, 073138 (2020)
21. J.D. Briers, S. Webster, J. Biomed. Opt. **1**, 174 (1996)
22. D.A. Boas, A.K. Dunn, J. Biomed. Opt. **15**, 011109 (2010)
23. P. Grassberger, *Information Dynamics*, H. Atmanspacher, H. Scheingraber, Eds., Plenum Press, New York, p. 15(1991)
24. A.L. Goldberger, L.A. Nunes Amaral, L. Glass, J.M. Hausdorff, P.Ch. Ivanov, R.G. Mark, J.E. Mietus, G.B. Moody, C.-K. Peng, H.E. Stanley, Circulation **101**(23), (2000) e215, http://circ.ahajournals.org/cgi/content/full/101/23/e215
25. K. Hu, P.Ch. Ivanov, Z. Chen, P. Carpena, H.E. Stanley, Phys. Rev. E **64**, 011114 (2001)
26. Z. Chen, P.Ch. Ivanov, K. Hu, H.E. Stanley, Phys. Rev. E **65**, 041107 (2002)
27. R.M. Bryce, K.B. Sprague, Sci. Rep. **2**, 315 (2012)
28. Y.H. Shao, G.F. Gu, Z.Q. Jiang, W.X. Zhou, D. Sornette, Sci. Rep. **2**, 835 (2012)
29. N.S. Frolov, V.V. Grubov, V.A. Maksimenko, A. Lüttjohann, V.V. Makarov, A.N. Pavlov, E. Sitnikova, A.N. Pisarchik, J. Kurths, A.E. Hramov, Sci. Rep. **9**, 7243 (2019)
30. A.N. Pavlov, A.I. Dubrovsky, A.A. Koronovskii Jr., O.N. Pavlova, O.V. Semyachkina-Glushkovskaya, J. Kurths, Chaos Solitons Fractals **139**, 109989 (2020)

31. A.N. Pavlov, A.I. Dubrovskii, O.N. Pavlova, O.V. Semyachkina-Glushkovskaya, Appl. Sci. **11**, 1182 (2021)
32. E.N. Lorenz, J. Atmos. Sci. **20**, 130 (1963)
33. V.S. Anishchenko, A.N. Silchenko, I.A. Khovanov, Phys. Rev. E **57**, 316 (1998)
34. D.D. Duncan, S.J. Kirkpatrick, R.K. Wang, J. Opt. Soc. Am. A **25**, 9 (2008)
35. A.S. Abdurashitov, V.V. Lychagov, O.A. Sindeeva, O.V. Semyachkina-Glushkovskaya, V.V. Tuchin, Front. Optoelectron. **8**, 187 (2015)
36. J. Zschocke, J. Leube, M. Glos, O. Semyachkina-Glushkovskaya, T. Penzel, R. Bartsch, J. Kantelhardt, IEEE Trans. Biomed. Eng. **69**, 830 (2022)
37. P.A. Dyachenko, A.S. Abdurashitov, O.V. Semyachkina-Glushkovskaya, V.V. Tuchin, in *Handbook of Tissue Optical Clearing: New Prospects in Optical Imaging*, CRC Press, p. 393(2022)
38. G.A. Guyo, A.N. Pavlov, E.N. Pitsik, N.S. Frolov, A.A. Badarin, V.V. Grubov, O.N. Pavlova, A.E. Hramov, Chaos Solitons Fractals **158**, 112038 (2022)
39. A.N. Pisarchik, A.E. Hramov, in *Multistability in Physical and Living Systems*, Springer, p. 255(2022)
40. N.S. Frolov, V.S. Khorev, V.V. Grubov, A.A. Badarin, S.A. Kurkin, V.A. Maksimenko, A.E. Hramov, A.N. Pisarchik, Chaos Solitons Fractals **158**, 112099 (2022)
41. O.N. Pavlova, G.A. Guyo, A.N. Pavlov, Phys. A **585**, 126406 (2022)
42. J. Alzahrani, H. Vaidya, K.V. Prasad, C. Rajashekhar, D.L. Mahendra, I. Tlili, Case Studies Thermal Eng. **34**, 102037 (2022)
43. I. Tlili, T. Alharbi, J. Build. Eng. **52**, 104328 (2022)
44. I. Tlili, S.M. Sajadi, D. Baleanu, F. Ghaemi, Sustain. Energy Technol. Assess. **52B**, 102100 (2022)
45. J. Zhang, S.M. Sajadi, Y. Chen, I. Tlili, M.A. Fagiry, Sustain. Energy Technol. Assess. **52B**, 102114 (2022)